J. Mech. Phys. Solids 191 (2024) 105784

Contents lists available at ScienceDirect

Journal of the Mechanics and Physics of Solids

journal homepage: www.elsevier.com/locate/jmps

A mechanics and electromagnetic scaling law for highly stretchable radio frequency electronics

Zichen Zhao[a,b,#], Raudel Avila[d,#], Dongjun Bai[a,c,#], Danli Xia[a,b], Enxi She[a,b], Yonggang Huang[e,f,g,h], John A. Rogers[e,f,i,j], Zhaoqian Xie[a,b,c,*]

[a] State Key Laboratory of Structural Analysis, Optimization and CAE Software for Industrial Equipment, Dalian University of Technology, Dalian 116024, China
[b] Department of Engineering Mechanics, Dalian University of Technology, Dalian 116024, China
[c] DUT-BSU Joint Institute, Dalian University of Technology, Dalian 116024, China
[d] Department of Mechanical Engineering, Rice University, Houston, TX 77005, United States
[e] Department of Materials Science and Engineering, Northwestern University, Evanston, IL 60208, United States
[f] Querrey Simpson Institute for Bioelectronics, Northwestern University, Evanston, IL 60208, United States
[g] Department of Mechanical Engineering, Northwestern University, Evanston, IL 60208, United States
[h] Departments of Civil and Environmental Engineering, Northwestern University, Evanston, IL 60208, United States
[i] Department of Biomedical Engineering, Northwestern University, Evanston, IL, United States
[j] Department of Neurological Surgery, Feinberg School of Medicine, Northwestern University, Chicago, IL, United States

ARTICLE INFO

Keywords:
Bio-integrated electronics
Near field communication antennas
Stretchable serpentines
Relative change of inductance
Strain

ABSTRACT

Many classes of flexible and stretchable bio-integrated electronic systems rely on mechanically sensitive electromagnetic components, such as various forms of antennas for wireless communication and for harvesting energy through coupling with external power sources. This efficient wireless functionality can be important for body area network technologies and can enable operation without the weight and bulky size of batteries for power supply. Recently, antenna designs have received increased attention because their mechanical and electromagnetic properties significantly influence the wireless performance of bio-integrated electronics, particularly under excessive mechanical loads. These mechanical factors are critical for skin-integrated electronics during human motion, as complex skin deformations can damage the conductive traces of antennas, such as those used for near-field communication (NFC), leading to yield or fracture and affecting their electromagnetic stability. Serpentine interconnects have been proposed as a geometric alternative to in-plane circular or rectangular spiral antenna designs to improve the elastic stretchability of the metallic traces in NFC antennas and prevent mechanical fractures. Despite the use of serpentine interconnects within the physiologically relevant strain range for skin (<20 %), the electromagnetic stability of the antennas decreases. This instability, reflected by shifts in resonance frequency and scattering parameters due to inductance changes, reduces the antennas' wireless power transfer efficiency and readout range. Therefore, maintaining the electromagnetic stability of antennas, specifically NFC antennas, under various mechanical deformations has become a critical challenge in practical wireless skin-integrated applications, such as sensing and physiological monitoring. Here, we establish a new mechanics and electromagnetic scaling law that quantifies the inductance changes under strain in a

* Corresponding author.
E-mail address: zxie@dlut.edu.cn (Z. Xie).
# These authors contributed equally to this work.

https://doi.org/10.1016/j.jmps.2024.105784
Received 30 June 2024; Received in revised form 9 July 2024; Accepted 11 July 2024
Available online 14 July 2024
0022-5096/© 2024 Elsevier Ltd. All rights are reserved, including those for text and data mining, AI training, and similar technologies.

rectangular-loop serpentine structure typically used for NFC wireless communication in stretchable electronics. We present a systematic analysis of the antenna's geometric parameters, material properties of the antenna and substrate, and the applied strain on the inductance change. Our findings demonstrate that the relative change of inductance is solely influenced by the serpentine structure's width-radius ratio, arc angle, aspect ratio of the NFC antennas, and the applied strain. Additionally, under physiological strain conditions for the skin, the relative change of inductance can be minimized to preserve the NFC antenna's performance and prevent mechanical fracture and electromagnetic stability loss.

1. Introduction

Mechanically deformable bioelectronic devices have enabled compelling applications in wireless, implanted or skin-mounted physiological monitors for health and well-being as well as those in electrical stimulation and drug release, functioning as conformal sensors capable of operating in anatomical areas subjected to complex deformations (Choi et al., 2021; Garland et al., 2023; Jung et al., 2022; Kim et al., 2024; S.H. Kim et al., 2024; Kwon et al., 2023; Oh et al., 2021; Ouyang et al., 2024; Stuart et al., 2023). These soft, bioelectronic devices rely on integrated antennas embedded within the electronics layout to transmit and receive data/-power from external devices wirelessly. A widely used protocol for establishing antenna communications through proximity (a few centimeters) in small devices is near field communication (NFC), where antennas operate at 13.56 MHz (An et al., 2024; Du, 2013; Wang et al., 2020). NFC antennas, which occupy a relatively small surface area, are typically found in contactless payment cards, identification tags, smartphones, and wearable devices (Dang et al., 2019; Du, 2013). However, these applications feature mechanically rigid designs where the antennas and electronic components do not deform. A significant mechanical advantage of recent flexible and stretchable electronic systems is their ability to seamlessly conform to the skin and other biological tissues for continuous bio-physical/biochemical signal sensing and monitoring (Kim et al., 2011; Wang et al., 2024, 2020; Zhang et al., 2023). This capability requires that the stretchable device, including antennas, deform to match the soft mechanics of biological tissues. These deformations challenge the performance of the electromagnetic components since changes to the initial antenna geometry alter its inductive properties and efficiency. In recent years, researchers in radio-frequency engineering for stretchable systems have explored several non-linear geometries, innovative mechanical manipulations of internal electronic circuits, and new substrate materials to preserve electromagnetic stability (S.H. Kim et al., 2024; Wang et al., 2021; Xu et al., 2021, 2024; Zhu et al., 2022).

One common strategy to improve the stretchability of thin-film structures under strain is to leverage geometric shapes to induce buckling. Recent examples of this approach include horseshoe serpentine structures (Pan et al., 2017; Xu et al., 2017; Zhang et al., 2014), origami and kirigami designs (Lu et al., 2023; Yan et al., 2016; Zhang et al., 2015; Y. Zhu et al., 2022), fractal curves (Fan et al., 2014; Ma and Zhang, 2016), and three-dimensional structures for buckling-induced assembly (Xue et al., 2020). Among these configurations, serpentine structures have been widely used in stretchable electronics as interconnects between rigid electronic islands housing sensors and chips (Zhang et al., 2014). Due to their highly stretchable mechanics, achieved through extensive theoretical, numerical, and experimental studies, serpentine structures are now also employed as radio-frequency antennas in stretchable electronics to withstand the deformations imposed by skin motion (Xie et al., 2018, 2020). Miniaturized stretchable patch antennas with serpentine structures have enabled wireless energy harvesting in implantable optogenetic devices for small animal models (Park et al., 2015). Demonstrations in humans include multi-turn epidermal NFC antennas for neonatal monitoring featuring ultra-thin designs that integrate easily with skin areas undergoing large deformations (Chung et al., 2019). Similarly, mesh serpentine layouts have been proposed to design stretchable microwave systems, including transmission lines, dipole antennas, and midfield phased surface antennas (Chang et al., 2017). Structurally, the serpentines can be carefully engineered, along with soft materials, for compact areas in portable electronics to match the mechanics of skin. These radiative elements, which are highly sensitive to deformations, are used for body network area sensing applications (Zhu et al., 2019), where the electromagnetic response is dependent on strain, as demonstrated for 3D serpentine structure antennas (Yan et al., 2017) and other serpentine structure far-field antennas (Kim et al., 2020).

In epidermal devices, the motion and deformation of the skin are closely coupled to the deformations experienced by stretchable devices, particularly the electronic components and metallic interconnects. Excessive deformations can lead to unstable electronic performance (Hussain et al., 2015; S.H. Kim et al., 2024). For NFC antennas, the critical parameter to control is inductance, which depends on the total antenna length and geometry. The resonance frequency of the antenna is determined by $f = \frac{1}{2\pi\sqrt{LC}}$, where L is the inductance and C is the capacitance (An et al., 2024; Kim et al., 2015). When stretched, the antenna's inductance increases, causing the resonance frequency to shift. Under very large deformations, inductance changes can completely detune the antenna, affecting the stability and wireless efficiency required for signal output in stretchable electronic applications (Kim et al., 2015). Retaining electromagnetic efficiency with minimal resonance frequency shift, while allowing deformation during skin movements, remains a major design challenge for stretchable antennas.

Current analysis of antenna geometries in stretchable electronics often focuses on either the mechanical or electromagnetic performance individually. However, these aspects are closely linked, as mechanical deformations influence electromagnetic properties. Specifically, the deformation of antennas alters their self and mutual inductance, depending on the type of deformation and the design of the NFC antenna (Xie et al., 2020). In existing research, there is little theoretical framework that considers both mechanics and electromagnetics to guide the design of NFC antennas, enabling them to maintain electromagnetic stability under large deformations. Most designs use multiple iterations of finite element analysis (FEA) to achieve stable electromagnetic characteristics of antennas

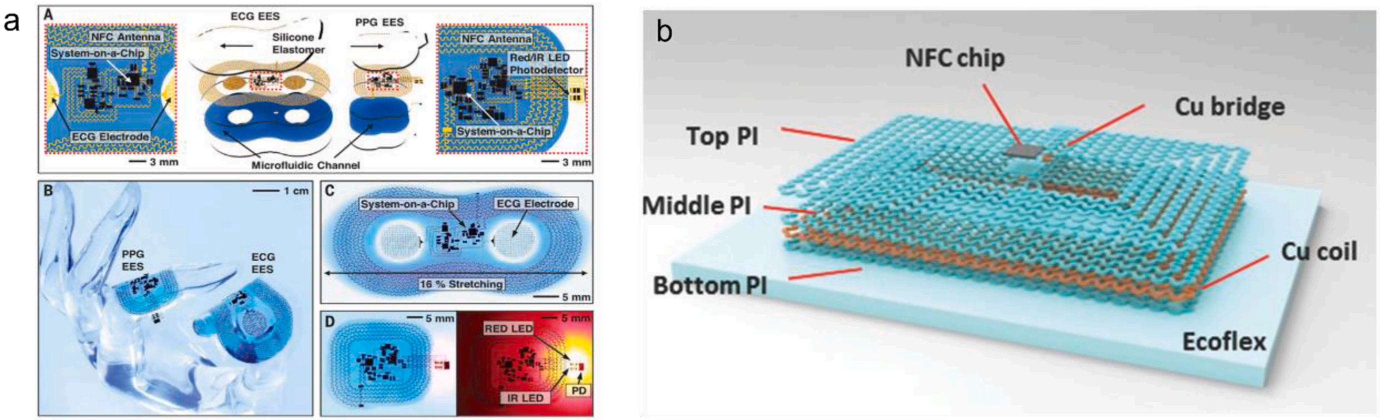

Fig. 1. (a) Diagram of binodal, wireless epidermal bioelectronic systems with in-sensor analytics for neonatal intensive care monitoring (Chung et al., 2019) Copyright 2019, AAAS, (b) 3D schematic view of the encapsulation and conductive material layers for a multi-turn rectangular NFC antenna on a flexible substrate (Kim et al., 2015) Copyright 2014, Wiley-VCH.

under large deformations, which is time-consuming (S.H. Kim et al., 2024). Therefore, it is necessary to propose a theoretical model to study the electromagnetic performance of NFC antennas undergoing large deformation and its influencing factors.

In this paper, based on our previous work (Fig. 1) (Chung et al., 2019; Kim et al., 2015), we propose a theoretical model to calculate the inductance change of the multi-turns rectangular NFC antennas composed of serpentine wires under strain. Finite element analysis is used to numerically solve the relative change of inductance, based on the total length change of the deformed antenna, for rectangular-loop antenna geometries using serpentine traces in wireless epidermal electronics (Fig. 1b). A new scaling law describes the relative change of inductance of the antennas through a combination of dimensionless parameters, providing design guidelines to minimize the inductance change under various strains for future stretchable electronic applications.

In the following sections, we present our study and corresponding scaling laws to model the relative change of inductance of rectangular serpentine antennas under strain, with relevant applications for near-field communication in stretchable electronics. First, in Section 2, we introduce the theoretical model for the electromagnetic analysis of multi-turn rectangular NFC antennas under strain. We also analyze the geometrical, material, and deformation variables that affect the antennas' relative change of inductance. Following this analysis, we establish a scaling law to quantify this relative change of inductance. Section 3 examines the effects of several dimensionless parameters within the scaling law formulation to model the relative change of inductance of serpentine antennas. We identify when specific parameters, or combinations of parameters, can be neglected or modified to obtain a more straightforward modeling framework for multi-turn antenna layouts. Finally, Section 4 discusses the optimal design of NFC antennas for practical stretchable electronic applications. We aim to minimize their relative change of inductance and maximize the mechanical stretchability under uniaxial or biaxial strains.

2. An electromagnetic model for serpentine antennas

An electromagnetic model is established for rectangular loop NFC antennas with horse-shoe serpentine designs to quantify the relative change of inductance under strain. Fig. 2 shows a schematic of an *N*-turn serpentine rectangular NFC antenna fully bonded to a low-modulus elastomer substrate and subjected to applied biaxial strains (ε_x and ε_y). The model is three-dimensional since the serpentine trace may buckle under strain, inducing out of plane deformation.

The parameters that may influence the inductance of the serpentine antennas can be classified into three categories that include:

1) Geometric parameters (Fig. 2), including the microscopic parameters for each unit of the horse-shoe serpentine trace: thickness (t) and width (w) in the cross section, radius (r), and arc angle (θ); and the macroscopic parameters: inner lengths (a_{in}, b_{in}), outer lengths (a_{out}, b_{out}), number of turns (N), and spacing (d).
2) Material parameters, including the Young's moduli, Poisson's ratios, and permeabilities of the substrate (E_{sub}, υ_{sub}, and μ_{sub}) and the serpentine trace (E_{ser}, υ_{ser}, and μ_{ser}), permeability μ_{air} of air, and permittivity ζ_{sub} of the substrate.
3) Applied strains ε_x and ε_y. For simplicity we neglect the effect of in-plane shear.
4) Let L_0 and L denote the inductances of the serpentine antenna before and after the applied strains, respectively. In general, the relationship between inductance L and the geometric, material, and deformation parameters can be expressed as

$$L = L\left(t, w, r, \theta, a_{\text{in}}, b_{\text{in}}, a_{\text{out}}, b_{\text{out}}, N, d, E_{\text{sub}}, E_{\text{ser}}, \nu_{\text{sub}}, \nu_{\text{ser}}, \mu_{\text{air}}, \mu_{\text{sub}}, \mu_{\text{ser}}, \zeta_{\text{sub}}, \varepsilon_x, \varepsilon_y\right) \tag{1}$$

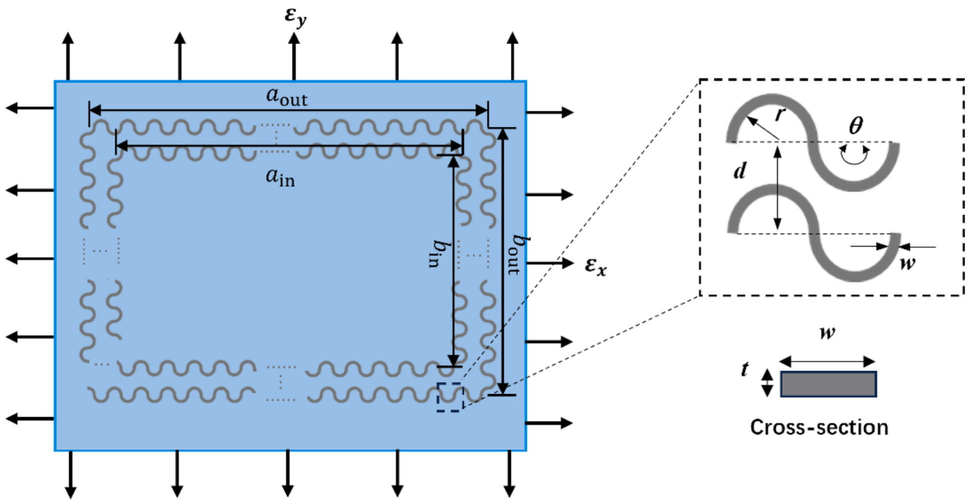

Fig. 2. Schematic of an *N*-turn rectangular loop antenna with serpentine traces on an elastomeric substrate subjected to biaxial strains.

First, a single-turn (N = 1) rectangular antenna is analyzed, for which the spacing d becomes irrelevant, and the macroscopic lengths can be rewritten as a and b. Eq. (1) becomes

$$L = L(t, w, r, \theta, a, b, E_{sub}, E_{ser}, \nu_{sub}, \nu_{ser}, \mu_{air}, \mu_{sub}, \mu_{ser}, \zeta_{sub}, \varepsilon_x, \varepsilon_y) \tag{2}$$

(It also depends on the frequency 13.56 MHz of the NFC antenna.) The baseline values for these parameters are $t = 5$ μm, $r = 125$ μm, $w = 50$ μm, $\theta = \pi$ (Kim et al., 2015), $E_{ser} = 119$ GPa and $\upsilon_{ser} = 0.34$ for copper (Xie et al., 2018), $E_{sub} = 69$ kPa and $\upsilon_{sub} = 0.48$ for Ecoflex, $\mu_{air} = \mu_{ser} = \mu_{sub} = 4\pi\times10^{-7}$ H/m (Babic and Akyel, 2020; Hu et al., 2022), and $\zeta_{sub} = 23.8 \times 10^{-12}$ F/m (Miranda et al., 2021).

Fig. 3 shows that the inductance of the NFC antenna does not depend on the permittivity ζ_{sub} of substrate within its common range 22×10^{-12}~31×10^{-12} F/m (Wen et al., 2018) such that ζ_{sub} does not appear in Eq. (2), i.e.,

$$L = L(t, w, r, \theta, a, b, E_{sub}, E_{ser}, \nu_{sub}, \nu_{ser}, \mu_{air}, \mu_{sub}, \mu_{ser}, \varepsilon_x, \varepsilon_y) \tag{3}$$

In addition, the permeabilities of serpentine traces, substrate, and air are the same (Babic and Akyel, 2020; Hu et al., 2022). The dimensional analysis shows that the inductance must be linearly proportional to μ_{ser} ($= \mu_{air} = \mu_{sub}$). The relative change of inductance, $\Delta L/L_0 = (L\text{-}L_0)/L_0$, becomes independent of μ_{ser} ($= \mu_{air} = \mu_{sub}$), and depends only on the 1) dimensionless geometric parameters t/r, w/r, θ, a/r, and a/b, 2) dimensionless material properties E_{sub}/E_{ser}, υ_{sub} and υ_{ser}, and 3) the applied strains. Eq. (3) can then be written via a non-dimensional function f as

$$\frac{\Delta L}{L_0} = f\left(\frac{t}{r}, \frac{w}{r}, \theta, \frac{a}{r}, \frac{a}{b}, \frac{E_{sub}}{E_{ser}}, \upsilon_{sub}, \upsilon_{ser}, \varepsilon_x, \varepsilon_y\right) \tag{4}$$

Its baseline values, based on previous serpentine antenna designs (Kim et al., 2015), are $t/r = 0.04$, $w/r = 0.4$, $\theta = \pi$, $a/r = 60$, $a/b = 1.5$, $E_{sub}/E_{ser} = 0.058\times10^{-5}$, $\upsilon_{sub} = 0.48$, $\upsilon_{ser} = 0.34$, $\varepsilon_x = 20$ %, and $\varepsilon_y = 0$. All subsequent discussions and results, unless otherwise noted, are based on these values.

3. Numerical results and a simplified scaling law

We study the influence of the dimensionless parameters on the relative change of inductance using the finite element analysis (see Appendix A for details). We first discuss the modulus ratio E_{sub}/E_{ser} for a single-turn rectangular-loop serpentine antenna. For copper traces (Young's modulus $E_{ser} = 119$ GPa) used in NFC antennas (Xie et al., 2018) on an elastomeric substrate (Young's modulus ranging from 69 kPa to 3 MPa (Cui et al., 2022; He et al., 2024), covering the human skin and commonly used silicone substrates), Figs. 4a, b and c show that the relative change of inductance $\Delta L/L_0$ is essentially independent of the modulus ratio E_{sub}/E_{ser} over its range of interest ($0.6 \times 10^{-6} < E_{sub}/E_{ser} < 2.5 \times 10^{-5}$) (Cui et al., 2022; Wang and Facchetti, 2019), and the Poisson's ratios of the substrate and serpentine, respectively. Therefore, Eq. (4) is further simplified to

$$\frac{\Delta L}{L_0} = L\left(\frac{t}{r}, \frac{w}{r}, \theta, \frac{a}{r}, \frac{a}{b}, \varepsilon_x, \varepsilon_y\right) \tag{5}$$

Among all geometric parameters, a/r is the only one representing the interplay between the macroscopic (a, b) and microscopic (t, w, r, θ) parameters. Fig. 5a shows that the $\Delta L/L_0 \sim a/r$ curve has an asymptote; for a/r beyond 60 (i.e., many units of horse-shoe serpentine trace along its length) as in most serpentine antennas, the relative change of inductance $\Delta L/L_0$ becomes independent of a/r. This fact of no interplay between the macroscopic and microscopic geometric parameters is further supported by Table 1, which shows that the dependence of the relative change of inductance $\Delta L/L_0$ on the macroscopic aspect ratio a/b of the NFC antenna and on the microscopic width w/r is completely decoupled, i.e., the function f in Eq. (5) is the product of one function of a/b and another function of w/r (and t/r and θ) within ~1.5 % error.

Fig. 5b shows that the relative change of inductance $\Delta L/L_0$ is linearly proportional to the applied strain ε_x (and $\varepsilon_y = 0$) for the macroscopic aspect ratio $a/b = 0.2$, 1.5, 5.0, at least for $\varepsilon_x < 20$ %. Similarly, it is also linearly proportional to ε_y (< 20 %) when the serpentine trace is stretched in the other direction (and $\varepsilon_x = 0$). Based on the results in Figs. 5a, 5b and Table 1, Eq. (5) can be written as

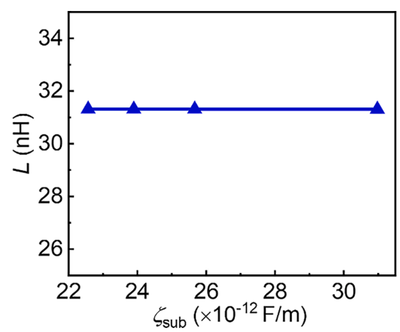

Fig. 3. The inductance as a function of the dielectric constant ζ_{sub} of substrate for the baseline parametric values of a single-turn serpentine antenna.

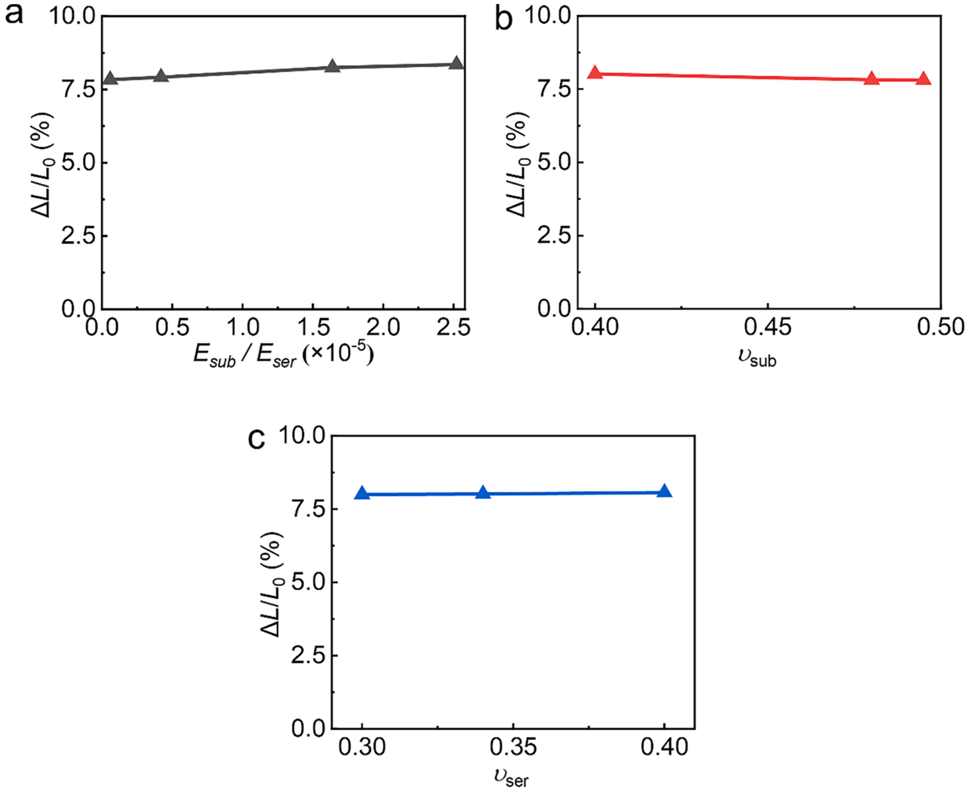

Fig. 4. The relative change of inductance versus (a) the substrate to serpentine modulus ratio E_{sub}/E_{ser}, (b) and (c) the Piossion's ratios of substrate υ_{sub} and serpentine υ_{ser}, respectively, for a single-turn serpentine antenna.

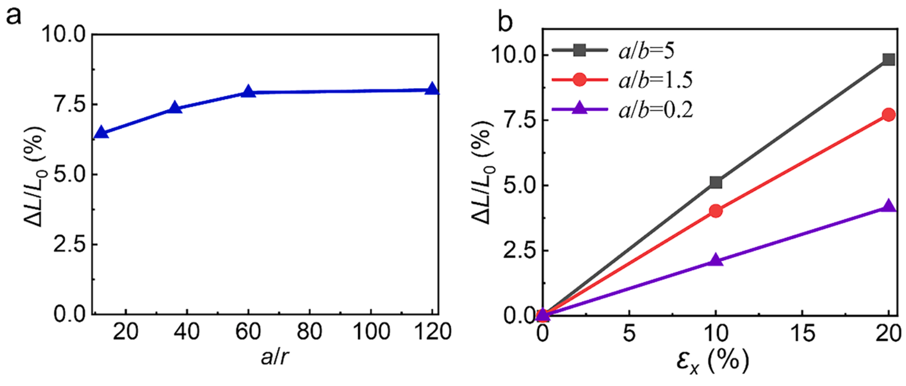

Fig. 5. The relative change of inductance versus (a) the ratio of macroscopic length a to microscopic radius r of the serpentine trace; and (b) the applied strain ε_x for several macroscopic aspect ratios a/b of the NFC antenna.

Table 1
The relative change of inductance $\Delta L/L$ versus with different a/b and w/r.

	$w/r = 0.2$	$w/r = 0.3$	$w/r = 0.4$	$w/r = 0.5$	$w/r = 0.6$
$a/b = 0.5$	0.0477	0.0495	0.0537	0.0579	0.0629
$a/b = 1$	0.0610	0.0637	0.0677	0.0727	0.0788
$a/b = 1.5$	0.0695	0.0722	0.0767	0.0824	0.0893

$$\frac{\Delta L}{L_0} = k_{\mathrm{micro}}\left(\frac{t}{r}, \frac{w}{r}, \theta\right) \cdot \left[k_{\mathrm{macro}}\left(\frac{a}{b}\right)\varepsilon_x + k_{\mathrm{macro}}\left(\frac{b}{a}\right)\varepsilon_y\right] \tag{6}$$

where $k_{\text{macro}}(a/b)$ represents the influence of macroscopic aspect ratio a/b and is shown in Fig. 6; without losing generality we define $k_{\text{macro}}(1) = 1$; it has the interesting property of $k_{\text{macro}}(a/b) + k_{\text{macro}}(b/a) = 2$, the limits $k_{\text{macro}}(0) = 1/2$ and $k_{\text{macro}}(\text{infinity}) = 3/2$, and is well represented by the following expression (Fig. 6)

$$k_{\text{macro}} = 1 + \frac{1}{2}\tanh\left[0.29\left(\frac{a}{b} - \frac{b}{a}\right)\right] \tag{7}$$

$k_{\text{micro}}(t/r,\ w/r,\ \theta)$ represents the influence of microscopic parameters and is shown in Figs. 7a, 7b and 7c versus t/r, w/r, and θ, respectively. Fig. 7a clearly shows that the dimensionless thickness t/r has a negligible effect in k_{micro} within its representative range 0.016 and 0.064 (Kim et al., 2015). Therefore, Eq. (6) is further simplified to yield the following scaling law

$$\frac{\Delta L}{L_0} = k_{\text{micro}}\left(\frac{w}{r}, \theta\right) \cdot \left[k_{\text{macro}}\left(\frac{a}{b}\right)\varepsilon_x + k_{\text{macro}}\left(\frac{b}{a}\right)\varepsilon_y\right] \tag{8}$$

For the commonly used angle $\theta = \pi$, k_{micro} is well represented by (Fig. 7b)

$$k_{\text{micro}}\left(\frac{w}{r}, \pi\right) = 0.27\left(\frac{w}{r}\right)^2 + 0.3 \tag{9}$$

The analysis above has focused exclusively on a single-turn serpentine antenna. In the following we study antennas with multiple-turns to effectively distribute the self-inductance along the antennas' total length; specifically to study the influence of the number of turns N and trace spacing between turns d. The macroscopic lengths are related by (Fig. 2)

$$b_{\text{out}} = b_{\text{in}} + 2(N-1)d \tag{10}$$

$$a_{\text{out}} = a_{\text{in}} + 2(N-1)d \tag{11}$$

We define the effective lengths a and b for a multi-turn antenna as

$$a = \frac{a_{\text{in}} + a_{\text{out}}}{2} \tag{12}$$

$$b = \frac{b_{\text{in}} + b_{\text{out}}}{2} \tag{13}$$

Fig. 8 presents the relative change of inductance versus the applied strain ε_x under two different loading conditions: uniaxial stretching (i.e., $\varepsilon_y = 0$) and equi-biaxial stretching ($\varepsilon_y = \varepsilon_x$). The relative change of inductance for a single-turn and a three-turn rectangular serpentine antenna have negligible differences for both uniaxial and equi-biaxial stretching. Therefore the scaling law in Eq. (8) can be applied to a multi-turn serpentine antenna as

$$\frac{\Delta L}{L_0} = k_{\text{micro}}\left(\frac{w}{r}, \theta\right) \cdot \left\{k_{\text{macro}}\left[\frac{a_{\text{in}} + (N-1)d}{b_{\text{in}} + (N-1)d}\right]\varepsilon_x + k_{\text{macro}}\left[\frac{b_{\text{in}} + (N-1)d}{a_{\text{in}} + (N-1)d}\right]\varepsilon_y\right\} \tag{14}$$

4. Optimization and discussions

The microscopic and macroscopic geometric parameters are optimized to 1) minimize the inductance change due to the applied strains, and 2) maximize the mechanical stretchability of NFC antennas. Fig. 7 suggests that wire thickness t has no effect on the inductance change, and a small wire width w and large arc angle θ reduce k_{micro} therefore the inductance change. Meanwhile a small t, small w, and a large θ increase the mechanical stretchability (Xie et al., 2018; Zhang et al., 2014). Therefore they (small t, small w, and a large θ) achieve both minimal inductance change and maximal mechanical stretchability.

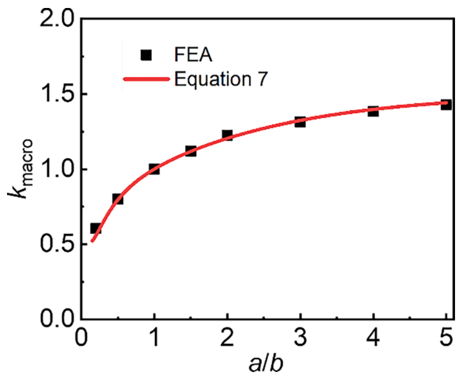

Fig. 6. k_{macro} versus the aspect ratio a/b of NFC antennas.

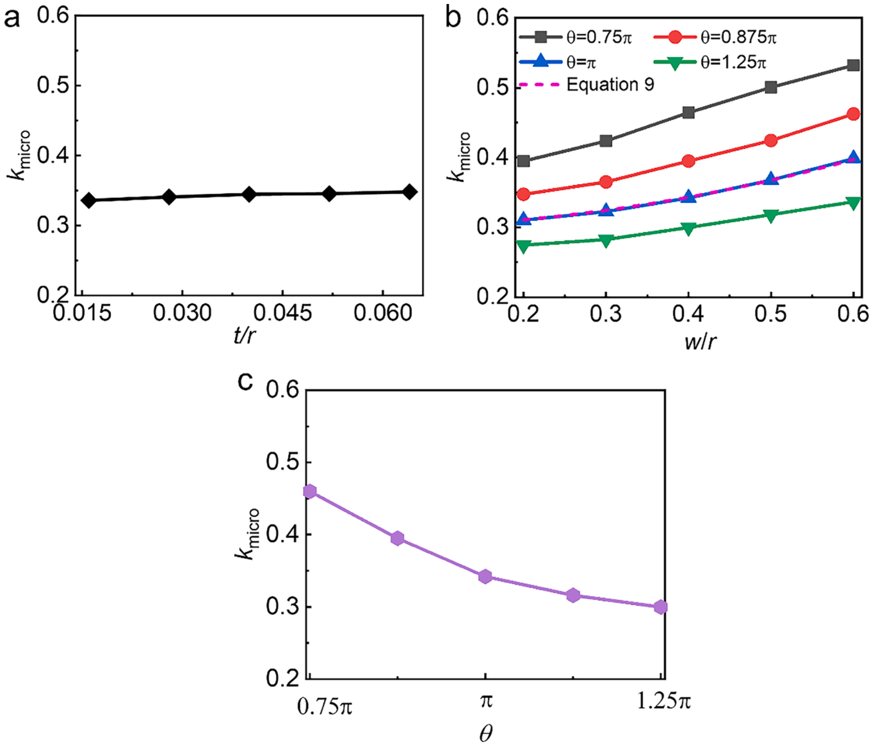

Fig. 7. k_{micro} versus (a) the dimensionless thickness t/r, (b) the dimensionless width w/r, and (c) the arc angle θ.

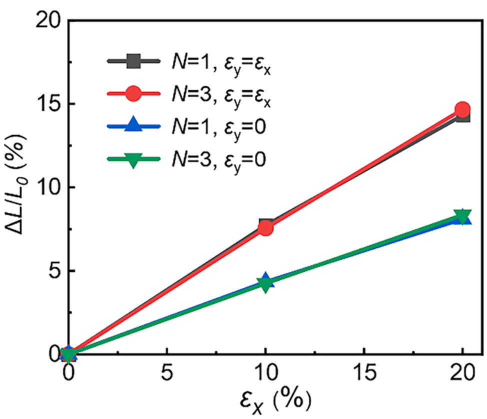

Fig. 8. The relative change of inductance for a single-turn and a three-turn rectangular serpentine antenna under uniaxial stretching ($\varepsilon_y = 0$) and equi-biaxial stretching (ε_y=ε_x).

The macroscopic lengths a and b do not affect the mechanical stretchability, but can be optimized to minimize the inductance change, though this optimization depends on the type of applied strain. For example,

1) Uniaxial stretching ε_x (and $\varepsilon_y = 0$): Eq. (8) becomes

$$\frac{\Delta L}{L_0} = k_{\mathrm{micro}}\left(\frac{w}{r}, \theta\right) \cdot k_{\mathrm{macro}}\left(\frac{a}{b}\right)\varepsilon_x \tag{15}$$

Therefore a small aspect ratio a/b is optimal since k_{macro} (therefore $\Delta L/L_0$) decreases monotonically with a/b.

2) Equi-biaxial stretching $\varepsilon_x = \varepsilon_y$: Eq. (8) becomes

$$\frac{\Delta L}{L_0} = 2k_{\text{micro}}\left(\frac{w}{r}, \theta\right)\varepsilon_x \tag{16}$$

It is independent of the aspect ratio a/b because k_{macro} has a unique property $k_{\text{macro}}(a/b) + k_{\text{macro}}(b/a) = 2$.

For general biaxial stretching (ε_x, ε_y), Eq. (8) can be used to optimize the aspect ratio a/b in order to minimize the inductance change. It is interesting to discuss the following two limits: 1) a square antenna: $a = b$ (for a single-turn antenna), or $a_{\text{in}}=b_{\text{in}}$ for a multiple-turn antenna; and 2) antenna with a very large number of turns N. Then Eq. (8) or Eq. (14) become

$$\frac{\Delta L}{L_0} = k_{\text{micro}}\left(\frac{w}{r}, \theta\right)\left(\varepsilon_x + \varepsilon_y\right) \tag{17}$$

It is linearly proportional to the change of antenna area $\varepsilon_x+\varepsilon_y$, as reported in the early studies (Kim et al., 2015). The coefficient of proportionality depends only on the dimensionless width w/r and arc angle θ through k_{micro}.

5. Conclusion

The inductance change of NFC antennas with serpentine structures is quantified under various strain fields using a new theoretical model, providing design guidelines for future mechanically insensitive stretchable electronics. This model includes a detailed analysis of mechanical and electromagnetic effects, considering geometrical, material, and mechanical parameters through a new scaling law that accurately captures the inductive response under strain. Numerical results indicate that for elastomeric substrates with a skin-like modulus of elasticity and thin-film NFC antenna serpentine geometries currently used in stretchable electronics, four dimensionless parameters mainly influence the inductance change: (1) serpentine width-radius ratio (e.g., given analytically in Eq. (9) for arc angle $\theta = \pi$), (2) arc angle, (3) antenna aspect ratio (as given analytically in Eq. (7)), and (4) (linearly proportional to the) applied strains. The results are also applicable to multi-turn serpentine antennas (as given in Eq. (14)). The established scaling law can be used to minimize the inductance change due to strain and maximize the mechanical stretchability, paving the way for future applications in highly stretchable yet electromagnetically stable technologies.

CRediT authorship contribution statement

Zichen Zhao: Investigation, Formal analysis, Methodology, Writing – original draft. **Raudel Avila:** Conceptualization, Writing – review & editing. **Dongjun Bai:** Investigation, Formal analysis, Methodology, Writing – original draft. **Danli Xia:** Formal analysis. **Enxi She:** Formal analysis. **Yonggang Huang:** Conceptualization, Writing – review & editing. **John A. Rogers:** Conceptualization, Writing – review & editing. **Zhaoqian Xie:** Conceptualization, Investigation, Formal analysis, Methodology, Funding acquisition, Writing – review & editing.

Declaration of competing interest

The authors declare that they have no known competing financial interests or personal relationships that could have appeared to influence the work reported in this paper.

Data availability

Data will be made available on request.

Acknowledgements

Zhaoqian Xie acknowledges support from the National Natural Science Foundation of China (12072057), Dalian Outstanding Young Talents in Science and Technology (2021RJ06). Raudel Avila acknowledges support from the ASME Haythornthwaite Foundation Research Initiation Grant and the Rice Provost's TMC Collaborator Fund.

Appendix A. Finite Element Analysis (FEA)

The finite element analysis (FEA) was conducted to study the inductance of the NFC antenna under given strain. Commercial software Abaqus was used to calculate the deformation of the NFC antennas. Eight-node 3D solid elements (C3D8R) and Four-node composite shell elements (S4R) were used for the substrate and serpentine traces, respectively. Convergence tests of the mesh size were performed to ensure accuracy. The deformed NFC antenna, obtained from mechanical simulation with commercial software Abaqus, was imported into the multiphysics analysis software COMSOL for the electromagnetic analyses, where the magnetic field and current-only models were adopted to calculate the inductance of the deformed NFC antenna at the general operating frequency 13.56 MHz of NFC antenna.

References

An, J., Yuen, C., Dai, L., Di Renzo, M., Debbah, M., Hanzo, L., 2024. Near-Field Communications: Research Advances, Potential, and Challenges. IEEe Wirel. Commun. 31 (3), 100–107. https://doi.org/10.1109/MWC.004.2300450.

Babic, S., Akyel, C., 2020. Self-Inductance of the Circular Coils of the Rectangular Cross-Section with the Radial and Azimuthal Current Densities. Physics. (College Park. Md) 2 (3), 352–367. https://doi.org/10.3390/physics2030019.

Chang, T., Tanabe, Y., Wojcik, C.C., Barksdale, A.C., Doshay, S., Dong, Z., Liu, H., Zhang, M., Chen, Y., Su, Y., Lee, T.H., Ho, J.S., Fan, J.A., 2017. A General Strategy for Stretchable Microwave Antenna Systems using Serpentine Mesh Layouts. Adv. Funct. Mater. 27 (46), 1703059 https://doi.org/10.1002/adfm.201703059.

Choi, Y.S., Yin, R.T., Pfenniger, A., Koo, J., Avila, R., Benjamin Lee, K., Chen, S.W., Lee, G., Li, G., Qiao, Y., Murillo-Berlioz, A., Kiss, A., Han, S., Lee, S.M., Li, C., Xie, Z., Chen, Y.Y., Burrell, A., Geist, B., Rogers, J.A., 2021. Fully implantable and bioresorbable cardiac pacemakers without leads or batteries. Nat. Biotechnol. 39 (10), 1228–1238. https://doi.org/10.1038/s41587-021-00948-x.

Chung, H.U., Kim, B.H., Lee, J.Y., Lee, J., Xie, Z., Ibler, E.M., Lee, K., Banks, A., Jeong, J.Y., Kim, J., Ogle, C., Grande, D., Yu, Y., Jang, H., Assem, P., Ryu, D., Kwak, J. W., Namkoong, M., Park, J.Bin, Rogers, J.A., 2019. Binodal, wireless epidermal electronic systems with in-sensor analytics for neonatal intensive care. Science (1979) 363 (6430), eaau0780. https://doi.org/10.1126/science.aau0780.

Cui, Z., Wang, W., Guo, L., Liu, Z., Cai, P., Cui, Y., Wang, T., Wang, C., Zhu, M., Zhou, Y., Liu, W., Zheng, Y., Deng, G., Xu, C., Chen, X., 2022. Haptically Quantifying Young's Modulus of Soft Materials Using a Self-Locked Stretchable Strain Sensor. Advanced Materials 34 (25), 2104078. https://doi.org/10.1002/adma.202104078.

Dang, F., Zhai, E., Li, Z., Zhou, P., Mohaisen, A., Bian, K., Wen, Q., Li, M., 2019. Pricing Data Tampering in Automated Fare Collection with NFC-Equipped Smartphones. IEEe Trans. Mob. Comput. 18 (5), 1159–1173. https://doi.org/10.1109/TMC.2018.2853114.

Du, H., 2013. NFC Technology: Today and Tomorrow. International Journal of Future Computer and Communication 2 (4), 351–354. https://doi.org/10.7763/IJFCC.2013.V2.183.

Fan, J.A., Yeo, W.H., Su, Y., Hattori, Y., Lee, W., Jung, S.Y., Zhang, Y., Liu, Z., Cheng, H., Falgout, L., Bajema, M., Coleman, T., Gregoire, D., Larsen, R.J., Huang, Y., Rogers, J.A., 2014. Fractal design concepts for stretchable electronics. Nat. Commun. 5 (1), 3266. https://doi.org/10.1038/ncomms4266.

Garland, N.T., Song, J.W., Ma, T., Kim, Y.J., Vázquez-Guardado, A., Hashkavayi, A.B., Ganeshan, S.K., Sharma, N., Ryu, H., Lee, M., Sumpio, B., Jakus, M.A., Forsberg, V., Kaveti, R., Sia, S.K., Veves, A., Rogers, J.A., Ameer, G.A., Bandodkar, A.J., 2023. A Miniaturized, Battery-Free, Wireless Wound Monitor That Predicts Wound Closure Rate Early. Adv. Healthc. Mater. 12 (28), 2301280 https://doi.org/10.1002/adhm.202301280.

He, D., Malu, D., Hu, Y., 2024. A Comprehensive Review of Indentation of Gels and Soft Biological Materials. Appl. Mech. Rev. 76 (5), 050802 https://doi.org/10.1115/1.4065434.

Hu, X., Liang, Z., Li, Q., Hu, S., Qu, S., 2022. Experimental study on the magnetic permeability of inclusion filled soft polymeric composite for soft-core transformer applications. Polym. Test. 106, 107430 https://doi.org/10.1016/j.polymertesting.2021.107430.

Hussain, A.M., Ghaffar, F.A., Park, S.I., Rogers, J.A., Shamim, A., Hussain, M.M., 2015. Metal/Polymer Based Stretchable Antenna for Constant Frequency Far-Field Communication in Wearable Electronics. Adv. Funct. Mater. 25 (42), 6565–6575. https://doi.org/10.1002/adfm.201503277.

Jung, Y.H., Yoo, J.Y., Vázquez-Guardado, A., Kim, J.H., Kim, J.T., Luan, H., Park, M., Lim, J., Shin, H.S., Su, C.J., Schloen, R., Trueb, J., Avila, R., Chang, J.K., Yang, D. S., Park, Y., Ryu, H., Yoon, H.J., Lee, G., Rogers, J.A., 2022. A wireless haptic interface for programmable patterns of touch across large areas of the skin. Nat. Electron. 5 (6), 374–385. https://doi.org/10.1038/s41928-022-00765-3.

Kim, D.H., Lu, N., Ma, R., Kim, Y.S., Kim, R.H., Wang, S., Wu, J., Won, S.M., Tao, H., Islam, A., Yu, K.J., Kim, T., Chowdhury, R., Ying, M., Xu, L., Li, M., Chung, H.J., Keum, H., McCormick, M., Rogers, J.A., 2011. Epidermal Electronics. Science (1979) 333 (6044), 838–843. https://doi.org/10.1126/science.1206157.

Kim, J., Banks, A., Cheng, H., Xie, Z., Xu, S., Jang, K.I., Lee, J.W., Liu, Z., Gutruf, P., Huang, X., Wei, P., Liu, F., Li, K., Dalal, M., Ghaffari, R., Feng, X., Huang, Y., Gupta, S., Paik, U., Rogers, J.A., 2015. Epidermal Electronics with Advanced Capabilities in Near-Field Communication. Small. 11 (8), 906–912. https://doi.org/10.1002/smll.201402495.

Kim, J., Bury, M.I., Kwon, K., Yoo, J.Y., Halstead, N.V., Shin, H.S., Li, S., Won, S.M., Seo, M.H., Wu, Y., Park, D.Y., Kini, M., Kwak, J.W., Madhvapathy, S.R., Ciatti, J. L., Lee, J.H., Kim, S., Ryu, H., Yamagishi, K., Rogers, J.A., 2024. A wireless, implantable bioelectronic system for monitoring urinary bladder function following surgical recovery. Proceedings of the National Academy of Sciences 121 (14), e2400868121. https://doi.org/10.1073/pnas.2400868121.

Kim, S.H., Basir, A., Avila, R., Lim, J., Hong, S.W., Choe, G., Shin, J.H., Hwang, J.H., Park, S.Y., Joo, J., Lee, C., Choi, J., Lee, B., Choi, K.S., Jung, S., Kim, T.Il, Yoo, H., Jung, Y.H, 2024. Strain-invariant stretchable radio-frequency electronics. Nature 629, 1047–1054. https://doi.org/10.1038/s41586-024-07383-3.

Kim, Y.S., Basir, A., Herbert, R., Kim, J., Yoo, H., Yeo, W.H., 2020. Soft Materials, Stretchable Mechanics, and Optimized Designs for Body-Wearable Compliant Antennas. ACS. Appl. Mater. Interfaces. 12 (2), 3059–3067. https://doi.org/10.1021/acsami.9b20233.

Kwon, K., Kim, J.U., Won, S.M., Zhao, J., Avila, R., Wang, H., Chun, K.S., Jang, H., Lee, K.H., Kim, J.H., Yoo, S., Kang, Y.J., Kim, J., Lim, J., Park, Y., Lu, W., Kim, T., Banks, A., Huang, Y., Rogers, J.A., 2023. A battery-less wireless implant for the continuous monitoring of vascular pressure, flow rate and temperature. Nat. Biomed. Eng. 7 (10), 1215–1228. https://doi.org/10.1038/s41551-023-01022-4.

Lu, L., Leanza, S., Zhao, R.R., 2023. Origami With Rotational Symmetry: A Review on Their Mechanics and Design. Appl. Mech. Rev. 75 (5), 050801 https://doi.org/10.1115/1.4056637.

Ma, Q., Zhang, Y., 2016. Mechanics of Fractal-Inspired Horseshoe Microstructures for Applications in Stretchable Electronics. J. Appl. Mech. 83 (11), 111008 https://doi.org/10.1115/1.4034458.

Miranda, I., Souza, A., Sousa, P., Ribeiro, J., Castanheira, E.M.S., Lima, R., Minas, G., 2021. Properties and Applications of PDMS for Biomedical Engineering: A Review. J. Funct. Biomater. 13 (1), 2. https://doi.org/10.3390/jfb13010002.

Oh, Y.S., Kim, J.H., Xie, Z., Cho, S., Han, H., Jeon, S.W., Park, M., Namkoong, M., Avila, R., Song, Z., Lee, S.U., Ko, K., Lee, J., Lee, J.S., Min, W.G., Lee, B.J., Choi, M., Chung, H.U., Kim, J., Rogers, J.A., 2021. Battery-free, wireless soft sensors for continuous multi-site measurements of pressure and temperature from patients at risk for pressure injuries. Nat. Commun. 12 (1), 5008. https://doi.org/10.1038/s41467-021-25324-w.

Ouyang, W., Kilner, K.J., Xavier, R.M.P., Liu, Y., Lu, Y., Feller, S.M., Pitts, K.M., Wu, M., Ausra, J., Jones, I., Wu, Y., Luan, H., Trueb, J., Higbee-Dempsey, E.M., Stepien, I., Ghoreishi-Haack, N., Haney, C.R., Li, H., Kozorovitskiy, Y., Rogers, J.A., 2024. An implantable device for wireless monitoring of diverse physio-behavioral characteristics in freely behaving small animals and interacting groups. Neuron 112 (11), 1764–1777. https://doi.org/10.1016/j.neuron.2024.02.020.

Pan, T., Pharr, M., Ma, Y., Ning, R., Yan, Z., Xu, R., Feng, X., Huang, Y., Rogers, J.A., 2017. Experimental and Theoretical Studies of Serpentine Interconnects on Ultrathin Elastomers for Stretchable Electronics. Adv. Funct. Mater. 27 (37), 1702589 https://doi.org/10.1002/adfm.201702589.

Park, S.Il, Brenner, D.S., Shin, G., Morgan, C.D., Copits, B.A., Chung, H.U., Pullen, M.Y., Noh, K.N., Davidson, S., Oh, S.J., Yoon, J., Jang, K.I., Samineni, V.K., Norman, M., Grajales-Reyes, J.G., Vogt, S.K., Sundaram, S.S., Wilson, K.M., Ha, J.S., Rogers, J.A., 2015. Soft, stretchable, fully implantable miniaturized optoelectronic systems for wireless optogenetics. Nat. Biotechnol. 33 (12), 1280–1286. https://doi.org/10.1038/nbt.3415.

Stuart, T., Jeang, W.J., Slivicki, R.A., Brown, B.J., Burton, A., Brings, V.E., Alarcón-Segovia, L.C., Agyare, P., Ruiz, S., Tyree, A., Pruitt, L., Madhvapathy, S., Niemiec, M., Zhuang, J., Krishnan, S., Copits, B.A., Rogers, J.A., Gereau, R.W., Samineni, V.K., Gutruf, P., 2023. Wireless, Battery-Free Implants for Electrochemical Catecholamine Sensing and Optogenetic Stimulation. ACS. Nano 17 (1), 561–574. https://doi.org/10.1021/acsnano.2c09475.

Wang, B., Facchetti, A., 2019. Mechanically Flexible Conductors for Stretchable and Wearable E-Skin and E-Textile Devices. Advanced Materials 31 (28), 1901408. https://doi.org/10.1002/adma.201901408.

Wang, K.N., Li, Z.Z., Cai, Z.M., Cao, L.M., Zhong, N.N., Liu, B., Zhou, K., Huo, F.Y., Cai, B., Bu, L.L., 2024. The applications of flexible electronics in dental, oral, and craniofacial medicine. Npj. Flex. Electron. 8 (1), 33. https://doi.org/10.1038/s41528-024-00318-y.

Wang, P., Hu, M., Wang, H., Chen, Z., Feng, Y., Wang, J., Ling, W., Huang, Y., 2020. The Evolution of Flexible Electronics: From Nature, Beyond Nature, and To Nature. Advanced Science 7 (20), 2001116. https://doi.org/10.1002/advs.202001116.

Wang, W., Wang, S., Rastak, R., Ochiai, Y., Niu, S., Jiang, Y., Arunachala, P.K., Zheng, Y., Xu, J., Matsuhisa, N., Yan, X., Kwon, S.K., Miyakawa, M., Zhang, Z., Ning, R., Foudeh, A.M., Yun, Y., Linder, C., Tok, J.B.H., Bao, Z., 2021. Strain-insensitive intrinsically stretchable transistors and circuits. Nat. Electron. 4 (2), 143–150. https://doi.org/10.1038/s41928-020-00525-1.

Wen, Z., Yang, J., Ding, H., Zhang, W., Wu, D., Xu, J., Shi, Z., Xu, T., Tian, Y., Li, X., 2018. Ultra-highly sensitive, low hysteretic and flexible pressure sensor based on porous MWCNTs/Ecoflex elastomer composites. Journal of Materials Science: Materials in Electronics 29 (24), 20978–20983. https://doi.org/10.1007/s10854-018-0242-3.

Xie, Z., Avila, R., Huang, Y., Rogers, J.A., 2020. Flexible and Stretchable Antennas for Biointegrated Electronics. Advanced Materials 32 (15), 1902767. https://doi.org/10.1002/adma.201902767.

Xie, Z., Ji, B., Huo, Q., 2018. Mechanics Design of Stretchable Near Field Communication Antenna With Serpentine Wires. J. Appl. Mech. 85 (4), 045001 https://doi.org/10.1115/1.4039102.

Xu, G., Yuan, L., Chen, X., Jia, W., Wang, M., Yang, L., Zhu, J., Cheng, H., 2021. Design of non-dimensional parameters in stretchable microstrip antennas with coupled mechanics-electromagnetics. Mater. Des. 205, 109721 https://doi.org/10.1016/j.matdes.2021.109721.

Xu, R., Lee, J.W., Pan, T., Ma, S., Wang, J., Han, J.H., Ma, Y., Rogers, J.A., Huang, Y., 2017. Designing Thin, Ultrastretchable Electronics with Stacked Circuits and Elastomeric Encapsulation Materials. Adv. Funct. Mater. 27 (4), 1604545 https://doi.org/10.1002/adfm.201604545.

Xu, Y., Ye, Z., Zhao, G., Fei, Q., Chen, Z., Li, J., Yang, M., Ren, Y., Berigan, B., Ling, Y., Qian, X., Shi, L., Ozden, I., Xie, J., Gao, W., Chen, P.Y., Yan, Z., 2024. Phase-separated porous nanocomposite with ultralow percolation threshold for wireless bioelectronics. Nat. Nanotechnol. https://doi.org/10.1038/s41565-024-01658-6.

Xue, Z., Song, H., Rogers, J.A., Zhang, Y., Huang, Y., 2020. Mechanically-Guided Structural Designs in Stretchable Inorganic Electronics. Advanced Materials 32 (15), 1902254. https://doi.org/10.1002/adma.201902254.

Yan, Z., Pan, T., Yao, G., Liao, F., Huang, Z., Zhang, H., Gao, M., Zhang, Y., Lin, Y., 2017. Highly stretchable and shape-controllable three-dimensional antenna fabricated by “Cut-Transfer-Release” method. Sci. Rep. 7 (1), 42227. https://doi.org/10.1038/srep42227.

Yan, Z., Zhang, F., Wang, J., Liu, F., Guo, X., Nan, K., Lin, Q., Gao, M., Xiao, D., Shi, Y., Qiu, Y., Luan, H., Kim, J.H., Wang, Y., Luo, H., Han, M., Huang, Y., Zhang, Y., Rogers, J.A., 2016. Controlled Mechanical Buckling for Origami-Inspired Construction of 3D Microstructures in Advanced Materials. Adv. Funct. Mater. 26 (16), 2629–2639. https://doi.org/10.1002/adfm.201504901.

Zhang, T., Liu, N., Xu, J., Liu, Z., Zhou, Y., Yang, Y., Li, S., Huang, Y., Jiang, S., 2023. Flexible electronics for cardiovascular healthcare monitoring. The Innovation 4 (5), 100485. https://doi.org/10.1016/j.xinn.2023.100485.

Zhang, Y., Wang, S., Li, X., Fan, J.A., Xu, S., Song, Y.M., Choi, K., Yeo, W., Lee, W., Nazaar, S.N., Lu, B., Yin, L., Hwang, K., Rogers, J.A., Huang, Y., 2014. Experimental and Theoretical Studies of Serpentine Microstructures Bonded To Prestrained Elastomers for Stretchable Electronics. Adv. Funct. Mater. 24 (14), 2028–2037. https://doi.org/10.1002/adfm.201302957.

Zhang, Y., Yan, Z., Nan, K., Xiao, D., Liu, Y., Luan, H., Fu, H., Wang, X., Yang, Q., Wang, J., Ren, W., Si, H., Liu, F., Yang, L., Li, H., Wang, J., Guo, X., Luo, H., Wang, L., Rogers, J.A., 2015. A mechanically driven form of Kirigami as a route to 3D mesostructures in micro/nanomembranes. Proceedings of the National Academy of Sciences 112 (38), 11757–11764. https://doi.org/10.1073/pnas.1515602112.

Zhu, J., Fox, J.J., Yi, N., Cheng, H., 2019. Structural Design for Stretchable Microstrip Antennas. ACS. Appl. Mater. Interfaces. 11 (9), 8867–8877. https://doi.org/10.1021/acsami.8b22021.

Zhu, J., Hu, Z., Zhang, S., Zhang, X., Zhou, H., Xing, C., Guo, H., Qiu, D., Yang, H., Song, C., Cheng, H., 2022. Stretchable 3D Wideband Dipole Antennas from Mechanical Assembly for On-Body Communication. ACS. Appl. Mater. Interfaces. 14 (10), 12855–12862. https://doi.org/10.1021/acsami.1c24651.

Zhu, Y., Schenk, M., Filipov, E.T., 2022. A Review on Origami Simulations: From Kinematics, To Mechanics, Toward Multiphysics. Appl. Mech. Rev. 74 (3), 030801 https://doi.org/10.1115/1.4055031.